

Achelous: A Fast Unified Water-surface Panoptic Perception Framework based on Fusion of Monocular Camera and 4D mmWave Radar

Runwei Guan^{1*}, Shanliang Yao^{1*}, Xiaohui Zhu², Ka Lok Man², Eng Gee Lim², Jeremy Smith¹, Yong Yue², Yutao Yue^{3*}

Abstract—Current perception models for different tasks usually exist in modular forms on Unmanned Surface Vehicles (USVs), which infer extremely slowly in parallel on edge devices, causing the asynchrony between perception results and USV position, and leading to error decisions of autonomous navigation. Compared with Unmanned Ground Vehicles (UGVs), the robust perception of USVs develops relatively slowly. Moreover, most current multi-task perception models are huge in parameters, slow in inference and not scalable. Oriented on this, we propose Achelous, a low-cost and fast unified panoptic perception framework for water-surface perception based on the fusion of a monocular camera and 4D mmWave radar. Achelous can simultaneously perform five tasks, detection and segmentation of visual targets, drivable-area segmentation, waterline segmentation and radar point cloud segmentation. Besides, models in Achelous family, with less than around 5 million parameters, achieve about 18 FPS on an NVIDIA Jetson AGX Xavier, 11 FPS faster than HybridNets, and exceed YOLOX-Tiny and Segformer-B0 on our collected dataset about 5 mAP₅₀₋₉₅ and 0.7 mIoU, especially under situations of adverse weather, dark environments and camera failure. To our knowledge, Achelous is the first comprehensive panoptic perception framework combining vision-level and point-cloud-level tasks for water-surface perception. To promote the development of the intelligent transportation community, we release our codes in <https://github.com/GuanRunwei/Achelous>.

Index Terms—Unified panoptic perception, Fusion of vision and radar, USV-based water-surface perception

I. INTRODUCTION

With the rapid development of deep learning, Autonomous Driving (AD) has been becoming highly intelligent. Perception, as an essential module of AD, assembles many environment perception tasks, including object detection, drivable-area segmentation, lane line segmentation, etc. Correspondingly, multi-sensor fusion has been applied to improve the precision and robustness of perception systems [1].

[◊]The authors acknowledge XJTLU-JITRI Academy of Industrial Technology for giving valuable support to the joint project. This work is supported by the Key Program Special Fund of XJTLU (KSF-A-19), Research Development Fund of XJTLU (RDF-19-02-23), Suzhou Science and Technology Fund (SYG202122). This work received financial support from Jiangsu Industrial Technology Research Institute (JITRI) and Wuxi National Hi-Tech District (WND).

*Runwei Guan and Shanliang Yao contribute equally.

¹Runwei Guan, Shanliang Yao and Jeremy Smith are with Faculty of Science and Engineering, University of Liverpool, L69 3BX Liverpool, United Kingdom. {runwei.guan, shanliang.yao, J.S.Smith}@liverpool.ac.uk

²Xiaohui Zhu, Ka Lok Man, Eng Gee Lim and Yong Yue are with School of Advanced Technology, Xi'an Jiaotong-Liverpool University, 215123 Suzhou, China. {xiaohui.zhu, Ka.Man, enggee.lim, yong.yue}@xjtlu.edu.cn

^{3*}Yutao Yue, corresponding author, is with Institute of Deep Perception Technology, JITRI, 214000 Wuxi, China. yueyutao@idpt.org

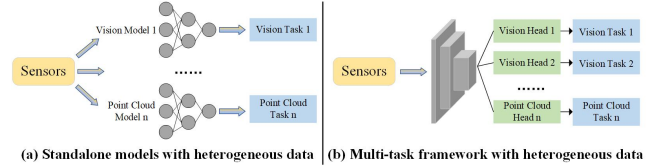


Fig. 1. Comparison of (a) standalone models and (b) multi-task framework with heterogeneous sensor data. Our Achelous belongs to the latter.

We have witnessed a remarkable development of unmanned ground vehicles (UGVs) with the help of deep learning. However, water-surface perception develops considerably slowly compared with road perception. Unmanned surface vehicles (USVs) play a significant role in water handling, such as water rescue [2], water quality monitoring [3], garbage collection [4] and geological exploration [5]. Based on extensive surveys, firstly, we find most models of water-surface perception can only execute a single task [6][7][8], which is far to help USVs complete autonomous navigation. In addition, some researches show that multi-tasks can improve each other [9][10]. Secondly, the industry prefers to parallelize multiple single-task models, which may lead to asynchronous perception results. Besides, perception system speed depends on the slowest model (Fig. 1). Thirdly, many models have never considered the problem of real-time inference on edge devices. They can only run on high-performance GPU devices [9][11] at remote servers, which excessively relies on network communication capabilities. However, the network communication is weakened dramatically during ocean voyages, once the network is interrupted, it may be a catastrophe for USVs during some dangerous tasks. Last but not least, vision-only models [12][13] are unreliable when confronted with dark environments, dense fog or lens failure. Currently, 4D mmWave radar is considered a promising complementary perception sensor for cameras in adverse situations, but how to efficiently extract irregular radar features is a challenge. Based on the above,

- 1) We propose Achelous (Fig. 2), a low-cost and fast unified water-surface panoptic perception framework based on the fusion of a monocular camera and 4D radar. Achelous ensembles five perception tasks in one end-to-end framework, including object detection, object semantic segmentation, waterline segmentation, drivable-area segmentation and radar point cloud semantic segmentation. Achelous obtains about 18 FPS on an NVIDIA Jetson AGX Xavier and achieves

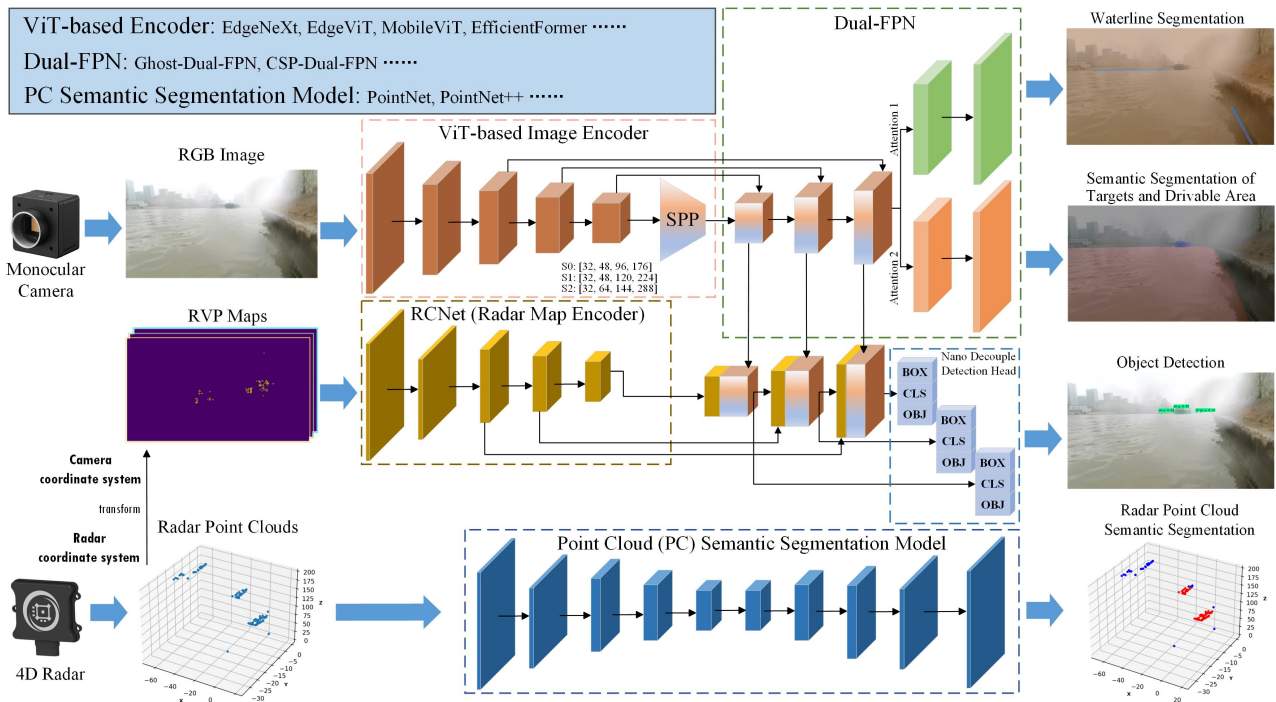


Fig. 2. The architecture of Achelous. Blue point clouds in the semantic segmentation of radar point clouds denote clutter while the red one denotes target.

TABLE I
COMPARISON OF PANOPTIC PERCEPTION MODELS (FRAMEWORKS)

Name	Type ¹	Sensor(s)	Tasks	Edge Test	Scalable
YOLOP [11]	M	camera	3	✗	✗
HybridNets [9]	M	camera	3	✗	✗
Achelous (ours)	F	camera 4D radar	5	✓	✓

1. Model or Framework.

competitive performances compared with single-task models and other multi-task models on perception tasks.

- 2) We propose a simple but effective convolution operator called Radar Convolution (RadarConv). RadarConv is friendly to the irregularness of radar point clouds and can meticulously and effectively extract point cloud features in 2D image planes, compared with the normal convolution.
- 3) To promote the development of water-surface panoptic perception based on multiple sensors, our Achelous family are scalable and open-source.

II. ACHELOUS

A. Overview

As Fig. 2 presents, our Achelous is based on a USV mounted with a monocular camera and 4D radar. The monocular camera captures RGB images while 4D radar obtains 3D point clouds directly. Each radar point cloud contains several physical features of targets. Among these physical features, we select the range, velocity and reflected power of

the target, which cannot be perceived by the camera. To make radar point clouds assist vision-based object detection, we transform the coordinates of point clouds from the 3D radar coordinate system to 2D camera plane. We call 2D radar pseudo images RVP maps, where each channel represents the radar target’s range, velocity and power.

The main body of our Achelous contains four parts, a ViT-based image encoder, a radar feature encoder, prediction heads and a point cloud semantic segmentation model. As Table I presents, our Achelous supports more sensors and tasks than the other two panoptic perception models, YOLOP and HybridNets. Besides, Achelous specifically performs edge test, where the modules are optional and scalable. Achelous has three channel sizes, S0, S1 and S2. To accelerate inference, Achelous compresses branches and network fragmentation as much as possible, and weighs uses of activation function and group convolution. Besides, Achelous keep input and output channels of network unit equal to reduce memory access cost.

B. ViT-based Image Encoder

We have witnessed excellent performances of vision-transformer-based (ViT-based) models over the past years. ViT-based models can model global contextual features based on the self-attention mechanism [14]. In addition, ViTs overall exceed CNNs in predictive performances [15][16][17]. ViTs are more robust than CNNs on adversarial attacks [18][19][20], vision object occlusions [21] and data corruptions [22]. Multi-head self-attention can assemble prediction features but CNNs cannot [23], whose information capacity is much more than CNNs with the same parameters. Although ViTs are blamed for slow inference, recent studies

[24][25][26][27] indicate that ViTs with ingenious design can still run as fast as CNNs. Based on the above advantages, our Achelous leverages ViT-based models as image encoders. Followed by the consistent paradigm of backbones, our image encoder has five stages with feature maps of multi-scale sizes, where the last four stages contain 2, 2, 6 and 4 layers, respectively. Our Achelous preliminarily contains four lightweight ViT-based backbones, EdgeNeXt [25], EdgeViT [24], MobileViT [26] and EfficientFormer [27]. Following the backbone, spatial pyramid pooling (SPP) [28] is to enlarge receptive fields of image feature maps with multiple scales.

C. Dual-FPN and Segmentation Heads

Feature Pyramid Network (FPN), as a significant module, is to fuse multi-scale features. Achelous has a dual FPN, fusing features extracted by the ViT-based encoder, where the first three feature maps are weight-shared and the last feature map is weight-independent. Between the weight-shared and weight-independent feature maps, we use two shuffle attention [29] modules to remeasure features of two different segmentation tasks. Inspired by GhostNet [30] and CSPDarknet [31], we design two lightweight FPNs, Ghost-Dual-FPN (GDF) and CSP-Dual-FPN (CDF), where GDF could dramatically remove feature redundancy in feature fusion stage while CDF could speed up feature fusion operations. Moreover, there are two segmentation heads following fused feature maps, which are for waterline segmentation, and semantic segmentation of targets and drivable-area.

D. Point Cloud Semantic Segmentation Model

Since cameras may fail due to awful weather, radar would take over the perception of Achelous. As radar could not adopt the vision-based detection pattern, semantic segmentation of radar point clouds matters. Based on the ideas of permutation invariance and local feature learning from PointNet [32] and PointNet++ [33], there are many models of point cloud processing. Here, to reduce the computation burden of the framework and make it fast, we adopt PointNet and PointNet++ as components of point cloud semantic segmentation. In addition, we reduce the number of channels of models to one-third of the original, because radar point clouds are dramatical sparser than lidars and too many latent channels are redundant.

E. Radar Convolution, RCBlock, RCNet and Fusion with Image Features

We notice that radar point clouds are sparse and irregular, which means the conventional convolution contains many invalid operations and takes feature maps as regular grids. To make convolution friendly to feature extraction of radar point clouds and alleviate feature loss, we propose radar convolution (Fig. 3), a simple but highly-efficiency convolution operator. We first adopt average pooling with 3×3 to enlarge the receptive field. Compared to max-pooling, average pooling can keep more feature information, aggregating local features. Besides, the pooling operation is

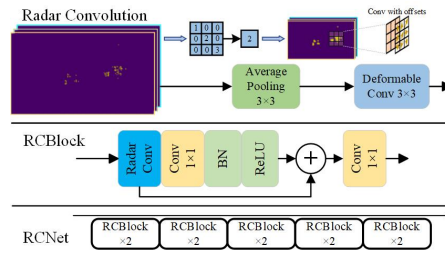


Fig. 3. Radar Convolution, RCBlock and RCNet.

much faster than convolution. To model the irregularity of radar point clouds, we introduce the deformable convolution [34], which extract feature with offsets. Based on radar convolution, we construct RCBlock and RCNet as shown in Fig. 3. RCBlock contains two 1×1 convolutions to weigh each spatial feature. The number of channels in RCNet is one-quarter of that in ViT-based image encoder, since radar point clouds are sparse and do not need so many latent features with non-linear operations.

RCNet is an auxiliary network for detection, where radar feature maps are concatenated to image feature maps in the dual-FPN, to help Achelous localize targets faster and improve the recall under adverse situations. Although many works fuse radar and image features in both backbone and neck [7][35], we find too many branches for fusion will cause a dramatic drop in inference speed. Since image feature maps in the dual-FPN contain abundant detailed low-level features for segmentation, in addition, upsampling operations and SPP equip feature maps with multi-scale features in different stages. Therefore, FPN-stage fusion is enough for robust object detection.

F. Nano Decouple Detection Head

We decouple feature maps in the detection head to predict bounding boxes, categories and confidence, respectively. In addition, we adopt depth-wise separable convolution to reduce parameters to a great extent. Furthermore, anchor-free is to accelerate inference and SimOTA [36] algorithm is to improve matching positive samples.

III. EXPERIMENTS

A. Experimental Settings

Device. We mount a SONY IMX-317 RGB camera and an Oculii EAGLE Imaging Radar on our USV. Sensors are temporally synchronized via timestamps and spatially synchronized via a calibration board.

Data. We capture 50,000 images and frames of radar data [41]. Each image is 1920×1080 pixels. There are seven classes for detection, including pier, buoy, sailor, ship, boat, vessel and kayak. Besides these classes, drivable area is an additional class for semantic segmentation while clutter is an additional class for point cloud semantic segmentation. Waterline is a single class for the waterline segmentation task. We annotate both object detection and semantic segmentation in VOC format. We annotate point cloud categories based on the ground truth of the bounding box and clustering by

TABLE II
PERFORMANCES OF ACHELOUS, OTHER MULTI-TASK MODELS AND SINGLE-TASK MODELS ON OUR TESTSET.

Methods	Sensors	TN ¹	Params (M)	FLOPs (G)	OD ²			SS ³		WS ⁴	PC-SS ⁵	FPS ¹⁴ _e	FPS ¹⁵ _g
					mAP ₅₀₋₉₅	mAP ₅₀	AR ₅₀₋₉₅	mIoU _t ¹²	mIoU _d ¹³	mIoU	mIoU		
Achelous-EN-CDF-PN-S0 ⁶	C ¹⁶ +R ¹⁷	5	3.59	5.38	37.2	66.3	43.1	68.1	98.8	69.4	57.1	17.5	59.8
Achelous-EN-GDF-PN-S0 ⁷	C+R	5	3.55	2.76	37.5	66.9	44.6	69.1	99.0	69.3	57.8	17.8	61.3
Achelous-EN-CDF-PN2-S0 ⁸	C+R	5	3.69	5.42	37.3	66.3	43.0	68.4	99.0	68.9	60.2	15.2	56.5
Achelous-EN-GDF-PN2-S0	C+R	5	3.64	2.84	37.7	68.1	45.0	67.2	99.2	67.3	59.6	14.8	57.7
Achelous-EF-GDF-PN-S0 ⁹	C+R	5	5.48	3.41	37.4	66.5	43.4	68.7	99.6	66.6	59.4	17.3	50.6
Achelous-EV-GDF-PN-S0 ¹⁰	C+R	5	3.79	2.89	38.8	67.3	42.3	69.8	99.6	70.6	58.0	16.4	54.9
Achelous-MV-GDF-PN-S0 ¹¹	C+R	5	3.49	3.04	41.5	71.3	45.6	70.6	99.5	68.8	58.9	16.0	53.7
Achelous-EN-GDF-PN-S1	C+R	5	5.18	3.66	41.3	70.8	45.5	67.4	99.4	69.3	58.8	16.6	59.7
Achelous-EF-GDF-PN-S1	C+R	5	8.07	4.52	40.0	70.2	43.8	68.2	99.3	68.7	58.2	16.6	46.8
Achelous-EV-GDF-PN-S1	C+R	5	4.14	3.16	41.0	70.7	45.9	70.1	99.4	67.9	59.2	16.7	56.6
Achelous-MV-GDF-PN-S1	C+R	5	4.67	4.29	43.1	75.8	47.2	73.2	99.5	69.2	59.1	15.8	55.8
Achelous-EN-GDF-PN-S2	C+R	5	6.90	4.59	40.8	70.9	44.4	69.6	99.3	71.1	59.0	16.1	58.1
Achelous-EF-GDF-PN-S2	C+R	5	14.64	7.13	40.5	70.8	44.5	70.3	99.1	71.7	58.4	13.5	39.3
Achelous-EV-GDF-PN-S2	C+R	5	8.28	5.19	40.3	69.7	43.8	74.1	99.5	67.9	58.3	14.7	47.1
Achelous-MV-GDF-PN-S2	C+R	5	7.18	6.02	45.0	79.4	48.8	73.8	99.6	70.8	58.5	15.6	52.7
YOLOP [11]	C	3	7.90	18.6	37.9	68.9	43.5	-	99.0	74.9	-	1.28	8.15
HybridNets [9]	C	3	12.83	15.6	39.1	69.8	44.2	-	98.8	71.5	-	6.04	17.1
YOLOv7-Tiny [37]	C	1	6.03	33.3	37.3	65.9	43.7	-	-	-	-	36.7	118.6
YOLOX-Tiny [36]	C	1	5.04	3.79	39.4	68.0	43.0	-	-	-	-	33.6	102.0
YOLOv4-Tiny [38]	C	1	5.89	4.04	13.1	36.3	20.2	-	-	-	-	114.6	352.2
Segformer-B0 [39]	C	1	3.71	5.29	-	-	-	72.5	99.2	72.1	-	41.6	124.7
PSPNet (MobileNet) [40]	C	1	2.38	2.30	-	-	-	69.4	99.0	69.7	-	61.2	246.1
PointNet [32]	R	1	3.53	1.19	-	-	-	-	-	-	59.0	97.0	507.4
PointNet++ [33]	R	1	1.88	2.63	-	-	-	-	-	-	60.7	72.8	384.2

1. TN: task number 2. OD: object detection 3. SS: semantic segmentation 4. WS: waterline segmentation 5. PC-SS: point cloud semantic segmentation 6. EN: EdgeNeXt, CDF: CSP-Dual-FPN, PN: PointNet 7. GDF: Ghost-Dual-FPN 8. PN2: PointNet++ 9. EF: EfficientFormer 10. EV: EdgeViT 11. MV: MobileViT 12. mIoU_t: mIoU of targets 13. mIoU_d: mIoU of drivable area 14. FPS_e: FPS on Jetson AGX Xavier 15. FPS_g: FPS on RTX A4000 16. C: camera 17. R: radar.

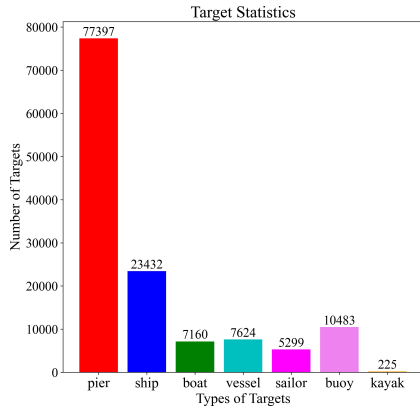


Fig. 4. Statistics of our collected dataset.

velocity. We divide data into the training, validation and test set by the ratio of 7:2:1.

Training and Evaluation. We resize images and RVP maps to 320×320 pixels. We train our Achelous for 100 epochs with a batch size of 32 and an initial learning rate of 0.03. We adopt Stochastic Gradient Descent (SGD) with a momentum of 0.937 as the optimizer and cosine learning rate scheduler. We use mixed precision and Exponential Moving Average (EMA) during training. We use the homoscedastic-uncertainty-based [10] multi-task training strategy. We adopt focal loss in detection, dice loss in segmentation and NLL

TABLE III
CONFIGURATION OF NVIDIA JETSON AGX XAVIER

Modules	Specifications
Memory	8 GB
CUDA Cores	384 NVIDIA CUDA cores + 48 Tensor cores
CPU	6-core ARM v8.2 64-bit
DLA	4.1 TFLOPS (FP16) + 8.2 TOPS (INT8)

loss in point cloud segmentation. We train Achelous and other models from scratch on two RTX A4000 GPUs with data-parallel mode. We test the FPS of all models on an NVIDIA Jetson AGX Xavier (TABLE III) and RTX A4000. We use mAP₅₀₋₉₅, mAP₅₀ and AR₅₀ as metrics to evaluate object detection while mIoU is to measure semantic segmentation of both image and radar point clouds.

B. Comparison of Achelous with Other Models

We compare our Achelous with other panoptic perception models and single-task models. We evaluate performances of object detection, target semantic segmentation, drivable area segmentation, waterline segmentation and point cloud semantic segmentation. We also test FPS on an edge device (NVIDIA Jetson AGX Xavier) and a high-performance GPU (RTX A4000). We observe that Achelous converges normally during multi-task training (Fig. 7). As Table II presents, our Achelous achieves state-of-the-art performances on object

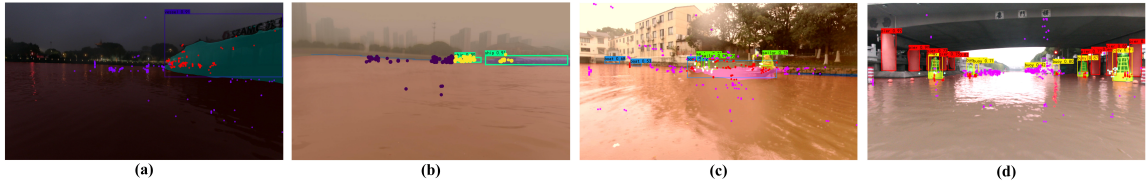


Fig. 5. Panoptic Perception Results of Achelous-EN-CDF-PN-S0, object detection, segmentation of targets, drivable area and waterline, and point cloud semantic segmentation. (a) Dark environment. (b) Occluded ships on a dense foggy day. (c) The lens blocked by water droplets. (d) Dense targets.

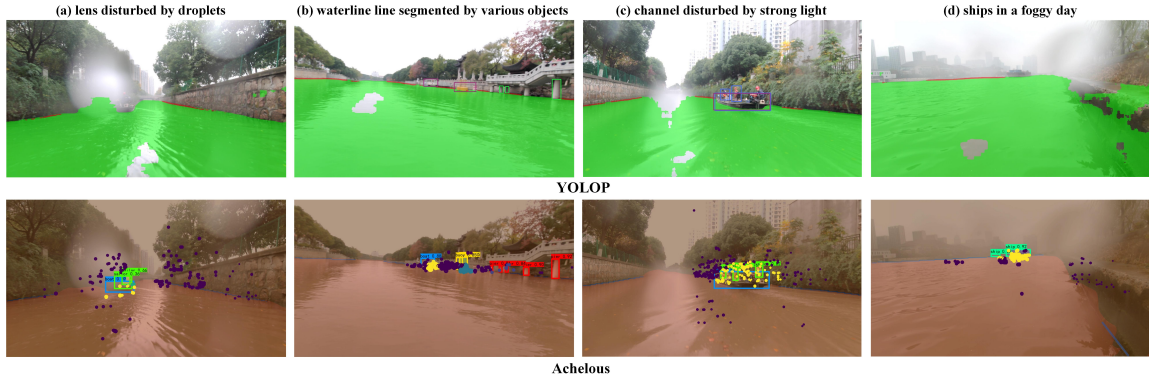


Fig. 6. Comparison of Achelous-MV-GDF-PN-S0 (4.4 million parameters less than YOLOP) with YOLOP under various situations.

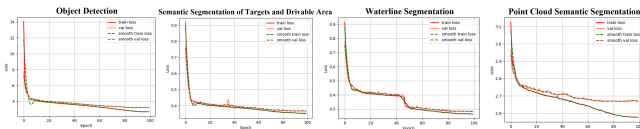


Fig. 7. Training and Validation Loss of Achelous-EN-GDF-PN2-S0.

detection, semantic segmentation of objects and drivable area compared with other panoptic perception models and single-task models. We observe that Achelous with the backbone of MobileViT achieves the best performance on object detection and semantic segmentation for three sizes (S0, S1 and S2), considerably outperforming other models. However, for waterline segmentation, YOLOP outperforms Achelous by about 3% mIoU. For point cloud semantic segmentation, Achelous with PointNet++ outperforms Achelous with PointNet. Furthermore, Achelous is much faster than YOLOP and HybridNets. The FPS of Achelous is between 13 to 18 on an NVIDIA Jetson AGX Xavier, which satisfies real-time inference for autonomous driving of USVs at a high speed.

We also visualize the prediction results of Achelous and YOLOP in Fig. 5 and Fig. 6. We can see in most circumstances, our Achelous can better detect and segment targets than YOLOP, no matter in dark environments, adverse weather or light interference.

C. Speed of Parallel Standalone Models and Achelous

As TABLE IV presents, we test the latency of standalone models of parallel inference and our Achelous-EN-GDF-PN-S0 on both Jetson AGX Xavier and RTX A4000. Our Achelous’s latency is lower than parallel standalone models when conducting several panoptic perception tasks, no matter

TABLE IV
INFERENCE SPEED OF STANDALONE MODELS AND ACHELOUS

Methods	Tasks	Latency _g ¹ (ms)	Latency _e ² (ms)
YOLOX-Tiny [36]	OD	21.2	79.5
Segformer-B0 [39]	SS		
PSPNet [40]	WS		
PointNet [32]	PC-SS		
Achelous (EN-GDF-PN-S0)	OD & SS WS & PS-SS	16.3 (↓ 4.9)	56.2 (↓ 23.3)

1. **Latency_g**: latency on a RTX A4000 GPU 2. **Latency_e**: latency on an NVIDIA Jetson AGX Xavier.

TABLE V
ABLATION EXPERIMENT OF RCNET AND FUSION METHODS

Methods	mAP ₅₀₋₉₅	mAP ₅₀
Achelous-MobileNetv2	37.2	66.0
Achelous-RCNet	37.5 (↑ 0.3)	66.6 (↑ 0.6)
Fusion Methods	mAP ₅₀₋₉₅	Latency _e (ms)
Backbone + Dual-FPN	37.4 ± 0.3	29.5
Dual-FPN	37.5 ± 0.2	16.3 (↓ 13.2)

on Jetson or RTX A4000. It proves that multi-task models are necessary for panoptic perception to improve efficiency.

D. Ablation Experiments

We first do the ablation experiment on RCNet (TABLE V), where we replace RCNet with MobileNetV2 in Achelous-EN-GDF-PN-S0, a structurally similar network consisting of normal convolutions. We notice that mAP₅₀₋₉₅ drops 0.2 while AP₅₀ drops about 0.5. It proves that RCNet containing Radar Convolution can better capture and model features of

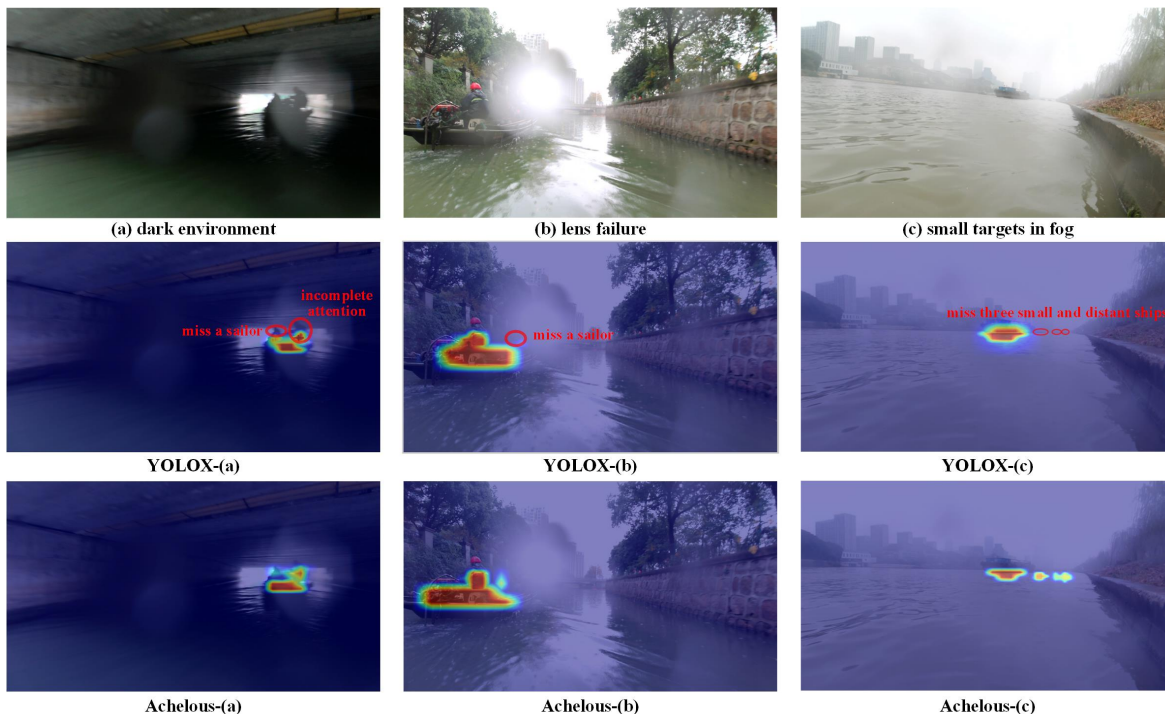


Fig. 8. Visualization of heatmaps of Achelous-MV-GDF-PN-S2 (7.2M parameters) and YOLOX-M (25.3M parameters) in different situations.

radar point clouds than the normal convolution calculator.

Furthermore, we compare the results of two different fusion methods. We find that fusion of image and radar features in both the backbone and fpn stage could not improve detection performances notably, whose inference latency is 13.2 ms slower than the fpn-level fusion.

E. Visualization and Analysis of Feature Maps

To validate whether our Achelous pays attention to correct regions of interest, we adopt Grad-CAM [42] to visualize the heatmaps of the last layer in FPN, which is connected with the detection head. We choose YOLOX-M to compare it with our Achelous-MV-GDF-PN-S2. We choose three challenging scenarios: a dark environment under the bridge, lens failure by droplet and a foggy day. Firstly, we observe that vision-only YOLOX-M performs terribly in the dark environment, where a sailor is missed and another is not focused precisely by YOLOX-M. Excitingly, Achelous with vision and radar features captures the distant sailor successfully. Secondly, when confronted with droplets on the lens, vision-only YOLOX-M completely ignore the targets in the region disturbed by droplets, but Achelous notices the ignored sailor. Thirdly, for the circumstance that three distant ships are obscured by the thick fog, our Achelous based on vision-radar fusion is aware of three small and distant ships but YOLOX-M is not, which validates the radar with long-range detection capability matters in some adverse weather. In all, Achelous based on the feature-level fusion of camera and 4D radar with fewer parameters is much more reliable than vision-only models during various challenging situations.

IV. CONCLUSION

We propose a powerful and scalable riverway panoptic perception framework called Achelous based on camera and 4D mmWave radar, which can simultaneously perform five different perception tasks of vision-level and point-cloud-level. Achelous is a high-efficiency framework, inferring in real-time on an NVIDIA Jetson AGX Xavier. We also propose radar convolution, which can exquisitely extract sparse and irregular features of radar point clouds. Achelous also outperforms other panoptic perception models and single-task models on most perception tasks, especially in adverse situations. We hope Achelous can promote the development of water-surface panoptic perception, providing a low-cost and high-efficiency scheme for researchers.

REFERENCES

- [1] Xuyang Bai, Zeyu Hu, Xinge Zhu, Qingqiu Huang, Yilun Chen, Hongbo Fu, and Chiew-Lan Tai, "Transfusion: Robust lidar-camera fusion for 3d object detection with transformers," in *Proceedings of the IEEE/CVF Conference on Computer Vision and Pattern Recognition*, 2022, pp. 1090–1099.
- [2] Tingting Yang, Zhi Jiang, Ruijin Sun, Nan Cheng, and Hailong Feng, "Maritime search and rescue based on group mobile computing for unmanned aerial vehicles and unmanned surface vehicles," *IEEE transactions on industrial informatics*, vol. 16, no. 12, pp. 7700–7708, 2020.
- [3] Xiaohui Zhu, Yong Yue, Prudence WH Wong, Yixin Zhang, and Hao Ding, "Designing an optimized water quality monitoring network with reserved monitoring locations," *Water*, vol. 11, no. 4, pp. 713, 2019.
- [4] Dario Madeo, Alessandro Pozzobon, Chiara Mocenni, and Duccio Bertoni, "A low-cost unmanned surface vehicle for pervasive water quality monitoring," *IEEE Transactions on Instrumentation and Measurement*, vol. 69, no. 4, pp. 1433–1444, 2020.

- [5] Zhibin Xue, Jincun Liu, Zhengxing Wu, Sheng Du, Shihan Kong, and Junzhi Yu, "Development and path planning of a novel unmanned surface vehicle system and its application to exploitation of qarhan salt lake," *Science China Information Sciences*, vol. 62, no. 8, pp. 1–3, 2019.
- [6] Mohammad-Hashem Haghbayan, Fahimeh Farahnakian, Jonne Poikonen, Markus Laurinen, Paavo Nevalainen, Juha Plosila, and Jukka Heikkonen, "An efficient multi-sensor fusion approach for object detection in maritime environments," in *2018 21st International Conference on Intelligent Transportation Systems (ITSC)*. IEEE, 2018, pp. 2163–2170.
- [7] Yuwei Cheng, Hu Xu, and Yimin Liu, "Robust small object detection on the water surface through fusion of camera and millimeter wave radar," in *Proceedings of the IEEE/CVF International Conference on Computer Vision*, 2021, pp. 15263–15272.
- [8] Keunhwan Kim, Jonghwi Kim, and Jinwhan Kim, "Robust data association for multi-object detection in maritime environments using camera and radar measurements," *IEEE Robotics and Automation Letters*, vol. 6, no. 3, pp. 5865–5872, 2021.
- [9] Dat Vu, Bao Ngo, and Hung Phan, "Hybridnets: End-to-end perception network," .
- [10] Alex Kendall, Yarin Gal, and Roberto Cipolla, "Multi-task learning using uncertainty to weigh losses for scene geometry and semantics," in *Proceedings of the IEEE conference on computer vision and pattern recognition*, 2018, pp. 7482–7491.
- [11] Dong Wu, Man-Wen Liao, Wei-Tian Zhang, Xing-Gang Wang, Xiang Bai, Wen-Qing Cheng, and Wen-Yu Liu, "Yolop: You only look once for panoptic driving perception," *Machine Intelligence Research*, p. 550–562, Nov 2022.
- [12] Lili Zhang, Yi Zhang, Zhen Zhang, Jie Shen, and Huibin Wang, "Real-time water surface object detection based on improved faster r-cnn," *Sensors*, vol. 19, no. 16, pp. 3523, 2019.
- [13] Tao Liu, Bo Pang, Lei Zhang, Wei Yang, and Xiaoqiang Sun, "Sea surface object detection algorithm based on yolo v4 fused with reverse depthwise separable convolution (rdsc) for usv," *Journal of Marine Science and Engineering*, vol. 9, no. 7, pp. 753, 2021.
- [14] Alexey Dosovitskiy, Lucas Beyer, Alexander Kolesnikov, Dirk Weissenborn, Xiaohua Zhai, Thomas Unterthiner, Mostafa Dehghani, Matthias Minderer, Georg Heigold, Sylvain Gelly, et al., "An image is worth 16x16 words: Transformers for image recognition at scale," in *International Conference on Learning Representations*.
- [15] Ze Liu, Yutong Lin, Yue Cao, Han Hu, Yixuan Wei, Zheng Zhang, Stephen Lin, and Baining Guo, "Swin transformer: Hierarchical vision transformer using shifted windows," in *Proceedings of the IEEE/CVF international conference on computer vision*, 2021, pp. 10012–10022.
- [16] Ze Liu, Han Hu, Yutong Lin, Zhuliang Yao, Zhenda Xie, Yixuan Wei, Jia Ning, Yue Cao, Zheng Zhang, Li Dong, et al., "Swin transformer v2: Scaling up capacity and resolution," in *Proceedings of the IEEE/CVF conference on computer vision and pattern recognition*, 2022, pp. 12009–12019.
- [17] Hangbo Bao, Li Dong, Songhao Piao, and Furu Wei, "Beit: Bert pre-training of image transformers," in *International Conference on Learning Representations*.
- [18] Rulin Shao, Zhouxing Shi, Jinfeng Yi, Pin-Yu Chen, and Cho-Jui Hsieh, "On the adversarial robustness of visual transformers," Mar 2021.
- [19] Srinadh Bhojanapalli, Ayan Chakrabarti, Daniel Glasner, Daliang Li, Thomas Unterthiner, and Andreas Veit, "Understanding robustness of transformers for image classification," Mar 2021.
- [20] Sayak Paul and Pin-Yu Chen, "Vision transformers are robust learners," *Proceedings of the AAAI Conference on Artificial Intelligence*, p. 2071–2081, Jul 2022.
- [21] MuhammadMuzammal Naseer, Kanchana Ranasinghe, SalmanH. Khan, Munawar Hayat, FahadShahbaz Khan, and Ming-Hsuan Yang, "Intriguing properties of vision transformers," Dec 2021.
- [22] Matthias Minderer, Josip Djolonga, Rob Romijnders, Frances Hubis, Xiaohua Zhai, Neil Houlsby, Dustin Tran, and Mario Lucic, "Revisiting the calibration of modern neural networks," *Advances in Neural Information Processing Systems*, vol. 34, pp. 15682–15694, 2021.
- [23] Namuk Park and Songkuk Kim, "Blurs behave like ensembles: Spatial smoothings to improve accuracy, uncertainty, and robustness," in *International Conference on Machine Learning*. PMLR, 2022, pp. 17390–17419.
- [24] Junting Pan, Adrian Bulat, Fuwen Tan, Xiatian Zhu, Lukasz Dudziak, Hongsheng Li, Georgios Tzimiropoulos, and Brais Martinez, "Edgevits: Competing light-weight cnns on mobile devices with vision transformers," in *Computer Vision–ECCV 2022: 17th European Conference, Tel Aviv, Israel, October 23–27, 2022, Proceedings, Part XI*. Springer, 2022, pp. 294–311.
- [25] Muhammad Maaz, Abdelrahman Shaker, Hisham Cholakkal, Salman Khan, Syed Waqas Zamir, Rao Muhammad Anwer, and Fahad Shahbaz Khan, "Edgenext: efficiently amalgamated cnn-transformer architecture for mobile vision applications," in *Computer Vision–ECCV 2022 Workshops: Tel Aviv, Israel, October 23–27, 2022, Proceedings, Part VII*. Springer, 2023, pp. 3–20.
- [26] Sachin Mehta and Mohammad Rastegari, "Mobilevit: light-weight, general-purpose, and mobile-friendly vision transformer," *arXiv preprint arXiv:2110.02178*, 2021.
- [27] Yanyu Li, Geng Yuan, Yang Wen, Ju Hu, Georgios Evangelidis, Sergey Tulyakov, Yanzhi Wang, and Jian Ren, "Efficientformer: Vision transformers at mobilenet speed," *Advances in Neural Information Processing Systems*, vol. 35, pp. 12934–12949, 2022.
- [28] Kaiming He, Xiangyu Zhang, Shaoqing Ren, and Jian Sun, "Spatial pyramid pooling in deep convolutional networks for visual recognition," *IEEE transactions on pattern analysis and machine intelligence*, vol. 37, no. 9, pp. 1904–1916, 2015.
- [29] Qing-Long Zhang and Yu-Bin Yang, "Sa-net: Shuffle attention for deep convolutional neural networks," in *ICASSP 2021 - 2021 IEEE International Conference on Acoustics, Speech and Signal Processing (ICASSP)*, May 2021.
- [30] Kai Han, Yunhe Wang, Qi Tian, Jianyuan Guo, Chunjing Xu, and Chang Xu, "Ghostnet: More features from cheap operations," in *2020 IEEE/CVF Conference on Computer Vision and Pattern Recognition (CVPR)*, Aug 2020.
- [31] Alexey Bochkovskiy, Chien-Yao Wang, and Hong-YuanMark Liao, "Yolov4: Optimal speed and accuracy of object detection," Apr 2020.
- [32] R. Qi Charles, Hao Su, Mo Kaichun, and Leonidas J. Guibas, "Pointnet: Deep learning on point sets for 3d classification and segmentation," in *2017 IEEE Conference on Computer Vision and Pattern Recognition (CVPR)*, Nov 2017.
- [33] CharlesR. Qi, Li Yi, Hao Su, and LeonidasJ. Guibas, "Pointnet++: Deep hierarchical feature learning on point sets in a metric space," Jun 2017.
- [34] Xizhou Zhu, Han Hu, Stephen Lin, and Jifeng Dai, "Deformable convnets v2: More deformable, better results," in *Proceedings of the IEEE/CVF conference on computer vision and pattern recognition*, 2019, pp. 9308–9316.
- [35] Yunyun Song, Zhengyu Xie, Xinwei Wang, and Yingquan Zou, "Ms-yolo: Object detection based on yolov5 optimized fusion millimeter-wave radar and machine vision," *IEEE Sensors Journal*, vol. 22, no. 15, pp. 15435–15447, 2022.
- [36] Zheng Ge, Songtao Liu, Feng Wang, Zeming Li, and Jian Sun, "Yolox: Exceeding yolo series in 2021," *arXiv preprint arXiv:2107.08430*, 2021.
- [37] Chien-Yao Wang, Alexey Bochkovskiy, and Hong-Yuan Mark Liao, "Yolov7: Trainable bag-of-freebies sets new state-of-the-art for real-time object detectors," *arXiv preprint arXiv:2207.02696*, 2022.
- [38] Alexey Bochkovskiy, Chien-Yao Wang, and Hong-Yuan Mark Liao, "Yolov4: Optimal speed and accuracy of object detection," *arXiv preprint arXiv:2004.10934*, 2020.
- [39] Enze Xie, Wenhai Wang, Zhiding Yu, Anima Anandkumar, Jose M Alvarez, and Ping Luo, "Segformer: Simple and efficient design for semantic segmentation with transformers," *Advances in Neural Information Processing Systems*, vol. 34, pp. 12077–12090, 2021.
- [40] Hengshuang Zhao, Jianping Shi, Xiaojuan Qi, Xiaogang Wang, and Jiaya Jia, "Pyramid scene parsing network," in *Proceedings of the IEEE conference on computer vision and pattern recognition*, 2017, pp. 2881–2890.
- [41] Shanliang Yao, Runwei Guan, Zhaodong Wu, Yi Ni, Zixian Zhang, Zile Huang, Xiaohui Zhu, Yutao Yue, Yong Yue, Hyungjoon Seo, and Ka Lok Man, "Waterscenes: A multi-task 4d radar-camera fusion dataset and benchmark for autonomous driving on water surfaces," 2023.
- [42] Ramprasaath R Selvaraju, Michael Cogswell, Abhishek Das, Ramakrishna Vedantam, Devi Parikh, and Dhruv Batra, "Grad-cam: Visual explanations from deep networks via gradient-based localization," in *Proceedings of the IEEE international conference on computer vision*, 2017, pp. 618–626.